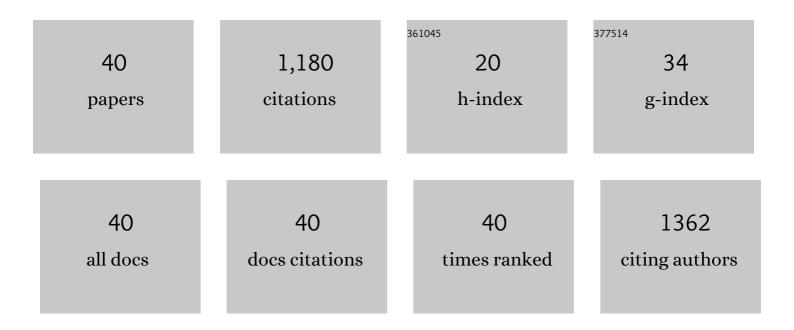
Issis C Romero-Ibarra

List of Publications by Year in descending order

Source: https://exaly.com/author-pdf/3192061/publications.pdf Version: 2024-02-01



#	Article	IF	CITATIONS
1	Experimental and theoretical analysis revealing the underlying chemistry accounting for the heterogeneous transesterification reaction in Na2SiO3 and Li2SiO3 catalysts. Renewable Energy, 2022, 184, 845-856.	4.3	6
2	Degradation of cefadroxil by photoelectrocatalytic ozonation under visible-light irradiation and single processes. Journal of Photochemistry and Photobiology A: Chemistry, 2022, 431, 113995.	2.0	4
3	Determination of active sites on Na2SiO3 and Li2SiO3 catalysts for methanol dissociation and methoxide stabilization concerning biodiesel production. Fuel, 2021, 298, 120840.	3.4	9
4	Pulse-Plating Electrodeposition of Metallic Bi in an Organic-Free Aqueous Electrolyte and Its Conversion into BiVO ₄ To Improve Photoelectrochemical Activity toward Pollutant Degradation under Visible Light. Journal of Physical Chemistry C, 2020, 124, 1421-1428.	1.5	10
5	Synthesis of sodium zincsilicate (Na2ZnSiO4) and heterogeneous catalysis towards biodiesel production via Box-Behnken design. Fuel, 2020, 280, 118668.	3.4	22
6	Unraveling the structural and composition properties associated with the enhancement of the photocatalytic activity under visible light of Ag2O/BiFeO3-Ag synthesized by microwave-assisted hydrothermal method. Applied Surface Science, 2020, 521, 146357.	3.1	27
7	In-situ transesterification of Jatropha curcas L. seeds using homogeneous and heterogeneous basic catalysts. Fuel, 2019, 235, 277-287.	3.4	62
8	Efficient cephalexin degradation using active chlorine produced on ruthenium and iridium oxide anodes: Role of bath composition, analysis of degradation pathways and degradation extent. Science of the Total Environment, 2019, 648, 377-387.	3.9	47
9	In situ synthesis of Au-decorated BiOCl/BiVO4 hybrid ternary system with enhanced visible-light photocatalytic behavior. Applied Surface Science, 2019, 487, 743-754.	3.1	32
10	In situ reactivation of spent NiMoP/γ-Al2O3 catalyst for hydrodesulfurization of straight-run gas oil. Catalysis Today, 2019, 329, 44-52.	2.2	6
11	A Facile Route to Synthesize a TiNT-RuO ₂ Electrocatalyst for Electro-Generated Active Chlorine Production. Journal of the Electrochemical Society, 2019, 166, H783-H790.	1.3	4
12	Molecular interactions arising in polyethyleneâ€bentonite nanocomposites. Journal of Applied Polymer Science, 2019, 136, 46920.	1.3	8
13	In search of the active chlorine species on Ti/ZrO2-RuO2-Sb2O3 anodes using DEMS and XPS. Electrochimica Acta, 2018, 275, 265-274.	2.6	26
14	The effect of different operational parameters on the electrooxidation of indigo carmine on Ti/IrO2-SnO2-Sb2O3. Journal of Environmental Chemical Engineering, 2018, 6, 3010-3017.	3.3	35
15	Microwaveâ€Assisted Solvothermal Oneâ€Pot Synthesis of RuO 2 Nanoparticles: First Insights of Its Activity Towards Oxygen and Chlorine Evolution Reactions. ChemistrySelect, 2018, 3, 12937-12945.	0.7	7
16	A novel green one-pot synthesis of biodiesel from Ricinus communis seeds by basic heterogeneous catalysis. Journal of Cleaner Production, 2018, 196, 340-349.	4.6	24
17	Key processing of porous and fibrous LaCoO3 nanostructures for successful CO and propane sensing. Ceramics International, 2018, 44, 15402-15410.	2.3	23
18	The Influence of Ni(II) and Co(II) Adsorptions in the Anomalous Behavior of Co-Ni Alloys: Density Functional Theory and Experimental Studies. ChemistrySelect, 2017, 2, 1826-1834.	0.7	7

#	Article	IF	CITATIONS
19	Controlling Li2CuO2 single phase transition to preserve cathode capacity and cyclability in Li-ion batteries. Solid State Ionics, 2017, 303, 89-96.	1.3	19
20	Thermal properties of centrifuged oils measured by alternative photothermal techniques. Thermochimica Acta, 2017, 657, 66-71.	1.2	14
21	CO2 adsorption at high pressures in MCM-41 and derived alkali-containing samples: the role of the textural properties and chemical affinity. Journal of Porous Materials, 2016, 23, 1155-1162.	1.3	4
22	First assessment of Li 2 O–Bi 2 O 3 ceramic oxides for high temperature carbon dioxide capture. Journal of Energy Chemistry, 2016, 25, 754-760.	7.1	10
23	Nanocomposite polymer electrolytes based on poly(poly(ethylene glycol)methacrylate), MMT or ZSM-5 formulated with LiTFSI and PYR ₁₁ TFSI for Li-ion batteries. RSC Advances, 2016, 6, 7249-7259.	1.7	11
24	Biodiesel production from soybean and Jatropha oils using cesium impregnated sodium zirconate as a heterogeneous base catalyst. Renewable Energy, 2016, 93, 323-331.	4.3	74
25	Li2SiO3 fast microwave-assisted hydrothermal synthesis and evaluation of its water vapor and CO2 absorption properties. Particuology, 2016, 24, 129-137.	2.0	16
26	Hierarchical Na-doped cubic ZrO2 synthesis by a simple hydrothermal route and its application in biodiesel production. Journal of Solid State Chemistry, 2014, 218, 213-220.	1.4	19
27	Influence of the Kâ€; Na―and Kâ€Naâ€carbonate additions during the CO ₂ chemisorption on lithium oxosilicate (Li ₈ SiO ₆). , 2014, 4, 145-154.		20
28	Sodium zirconate (Na2ZrO3) as a catalyst in a soybean oil transesterification reaction for biodiesel production. Fuel Processing Technology, 2014, 120, 34-39.	3.7	64
29	Thermodynamic and Kinetic Analyses of the CO ₂ Chemisorption Mechanism on Na ₂ TiO ₃ : Experimental and Theoretical Evidences. Journal of Physical Chemistry C, 2014, 118, 19822-19832.	1.5	37
30	CO2 Adsorption at Elevated Pressure and Temperature on Mg–Al Layered Double Hydroxide. Industrial & Engineering Chemistry Research, 2014, 53, 8087-8094.	1.8	27
31	CO2 capture properties of lithium silicates with different ratios of Li2O/SiO2: an ab initio thermodynamic and experimental approach. Physical Chemistry Chemical Physics, 2013, 15, 13538.	1.3	100
32	Microstructural and CO2 chemisorption analyses of Li4SiO4: Effect of surface modification by the ball milling process. Thermochimica Acta, 2013, 567, 118-124.	1.2	93
33	Analysis of the CO2 chemisorption reaction mechanism in lithium oxosilicate (Li8SiO6): a new option for high-temperature CO2 capture. Journal of Materials Chemistry A, 2013, 1, 3919.	5.2	69
34	Thermokinetic and microstructural analyses of the CO2 chemisorption on K2CO3–Na2ZrO3. Journal of CO2 Utilization, 2013, 3-4, 14-20.	3.3	17
35	Structural and CO ₂ Chemisorption Analyses on Na ₂ (Zr _{1–<i>x</i>} Al _{<i>x</i>})O ₃ Solid Solutions. Journal of Physical Chemistry C, 2013, 117, 16483-16491.	1.5	27
36	Li _{4+<i>x</i>} (Si _{1–<i>x</i>} Al _{<i>x</i>})O ₄ Solid Solution Mechanosynthesis and Kinetic Analysis of the CO ₂ Chemisorption Process. Journal of Physical Chemistry C, 2013, 117, 6303-6311.	1.5	52

#	Article	IF	CITATIONS
37	Influence of X-ray opaque BaSO4 nanoparticles on the mechanical, thermal and rheological properties of polyoxymethylene nanocomposites. Journal of Polymer Engineering, 2012, 32, 319-326.	0.6	12
38	Influence of the morphology of barium sulfate nanofibers and nanospheres on the physical properties of polyurethane nanocomposites. European Polymer Journal, 2012, 48, 670-676.	2.6	18
39	Hierarchically Nanostructured Barium Sulfate Fibers. Langmuir, 2010, 26, 6954-6959.	1.6	32
40	Mechanical and rheological studies on polyethylene terephthalate-montmorillonite nanocomposites. Polymer Engineering and Science, 2004, 44, 1094-1102.	1.5	86